applied sciences

MDPI

Article

Solvothermal Synthesis of Size-Controlled Monodispersed Superparamagnetic Iron Oxide Nanoparticles

Yongpeng Chen [1], Jianguo Zhang [1], Zhixin Wang [2] and Zunning Zhou [1,*]

[1] State Key Laboratory of Explosion Science and Technology, Beijing Institute of Technology, Beijing 100081, China; 3120195113@bit.edu.cn (Y.C.); zjgbit@bit.edu.cn (J.Z.)
[2] Army Aviation Institute, Beijing 101116, China; wzx98@126.com
* Correspondence: zzn@bit.edu.cn; Tel.: +86-10-68911202

Received: 7 November 2019; Accepted: 25 November 2019; Published: 28 November 2019

Abstract: Superparamagnetic iron oxide nanoparticles are of great interest in magnetic targeted drug delivery due to their unique properties. In this paper, size-controlled superparamagnetic iron oxide nanoparticles were synthesized in an ethylene glycol/diethylene glycol (EG/DEG) binary solvent system via a facile solvothermal method. X-ray diffraction (XRD), a scanning electron microscope (SEM), and a vibrating sample magnetometer (VSM) were used to confirm that the prepared samples were superparamagnetic Fe_3O_4 nanospheres. When the V_{EG}/V_{DEG} was varied from 100/0 to 80/20, 60/40, and 40/60, the average diameters of the resulting Fe_3O_4 nanospheres were approximately 700, 500, 300, and 100 nm, respectively. In addition, the saturation magnetization (M_s) of Fe_3O_4 nanoparticles with a size of 100, 300, 500, and 700 nm was 72.14, 75.94, 80.28, and 85.41 emu/g, and the corresponding remanent magnetization (M_r) was 3.34, 3.97, 3.26, and 4.28 emu/g, respectively. The relevant formation mechanisms of Fe_3O_4 nanoparticles are proposed at the end. These superparamagnetic Fe_3O_4 nanoparticles with high saturation magnetization may have use as targeted drug carriers.

Keywords: targeted drug delivery; superparamagnetic; size-controlled; solvothermal method

1. Introduction

Delivering a drug accurately and safely to its target site remains the yardstick for the design of drug delivery systems. Targeted drug delivery has attracted a significant amount of attention due to the unique advantage of precise control over a drug's release [1]. In particular, magnetic drug targeting is currently recognized as one of the most promising approaches to drug delivery [2–4]. A pharmaceutical drug is loaded onto the surface of the magnetic nanoparticles, which are released at the target site with an external localized magnetic field gradient, thereby achieving an accurate and targeted dose [5].

During the process of delivering magnetic drug-loaded nanoparticles, the magnetic force that is exerted on the particles plays a crucial role and is strongly dependent on the size of the particle [6]. Furthermore, the magnetic force is proportional to d^3, where d is the diameter of the particle [7]. In addition, to minimize the aggregation that is caused by the magnetic attractive forces, magnetic nanoparticles must have dependable superparamagnetic properties. As a result, superparamagnetic nanoparticles become magnetic in the presence of the external magnetic field, but revert to a nonmagnetic state that allows them to be excreted when the external magnetic field is removed [8]. Therefore, the size and superparamagnetism of magnetic nanoparticles are predominantly important to controlling the transport of a targeted drug.

Superparamagnetic iron oxide (Fe_3O_4) nanoparticles are frequently used as the drug carrier because of their low toxicity [9]. Among the reported synthetic methods, including ball-milling [10], co-precipitation [11,12], thermal decomposition [13,14], and microemulsion templating [15], the solvothermal method has been proven to be feasible for the synthesis of magnetic nanoparticles with a controllable morphology and microstructure [16–20]. A considerable amount of effort has been devoted to the size-controlled synthesis of magnetic nanoparticles, mainly focusing on changing the reaction time, temperature, surfactants, and the initial concentration of reagents [20–25]. However, despite these advances, the synthesis of size-controllable magnetic nanoparticles based on changing the solvent deserves further research.

In this study, size-tunable superparamagnetic Fe_3O_4 nanoparticles were synthesized via a facile solvothermal method based on a binary solvent system with ethylene glycol (EG) and diethylene glycol (DEG). To obtain superparamagnetic nanoparticles with a high saturation magnetization, polyvinyl pyrrolidone (PVP) and sodium citrate (Na_3Cit) were used together as structure guide agents. The Fe_3O_4 nanoparticles have nearly monodispersed sizes that are tunable in the range of 60–800 nm by varying the volume ratio of EG/DEG. The reaction mechanism of the solvothermal system is discussed. These superparamagnetic ferrite nanoparticles may be candidate targeted drug carriers.

2. Materials and Methods

2.1. Materials

Iron (III) chloride ($FeCl_3{\cdot}6H_2O$), sodium acetate (NaAc), K30 polyvinyl pyrrolidone (PVP), sodium citrate ($Na_3C_6H_5O_7{\cdot}2H_2O$, Na_3Cit), ethylene glycol (EG), and diethylene glycol (DEG) were purchased from Aladdin, Shanghai, China. All reagents were of analytical purity and used without further purification.

2.2. Synthesis of Nanoparticles

The monodispersed superparamagnetic iron oxide nanoparticles were synthesized by the solvothermal method. In a typical synthesis, 13 g $FeCl_3{\cdot}6H_2O$ was dissolved in 350 mL of ethylene glycol and diethylene glycol. Subsequently, 2 g NaAc, 2 g polyvinyl pyrrolidone (PVP), and sodium citrate (Na_3Cit) were added to the solution's ultrasonic processing. After an hour, the solution was sealed in a 400 mL Teflon-lined stainless-steel autoclave. The autoclave was heated to 210 °C for 12 h, and then cooled to room temperature naturally. The black products were collected by magnetic decantation and centrifugation, followed by repeated washing with deionized water and ethanol. The final products were dried in a vacuum oven at 50 °C for 12 h.

2.3. Characterization

A scanning electron microscope (SEM, JSM-7500F, Japan) and a transmission electron microscope (TEM, JEM 1200EX, Japan) were used to examine the structure of the samples. Phase analyses of the products were performed by X-ray diffraction (XRD, Bruker AXSD8 Advance, Germany) with Cu target radiation. The magnetic properties of the particles were measured at room temperature (298 K) using a vibrating sample magnetometer (VSM, Lake Shore7410, USA).

3. Results and Discussion

3.1. Structure and Morphology Analyses

Figure 1 shows the powder XRD patterns of the samples obtained with different ratios of V_{EG}/V_{DEG}. According to the patterns, all peaks of the four samples match well with those of standard Fe_3O_4 XRD diffraction (JCPDS Card No. 19-0629). Additionally, the intensity and full width at half maximum (FWHM) of the characteristic diffraction peaks are almost identical for the four samples. Table 1 shows the average crystal sizes of the Fe_3O_4 nanoparticles calculated using the Scherrer equation,

and the measurements of the FWHM of the (311) peaks. It is known that the superparamagnetic limit for magnetite is ~20 nm [26–28]. Hence, the as-prepared Fe_3O_4 nanoparticles may have satisfactory superparamagnetism, because the grain size of the samples is close to 20 nm (23.62 nm, 25.25 nm, 25.65 nm, 27.86 nm, respectively).

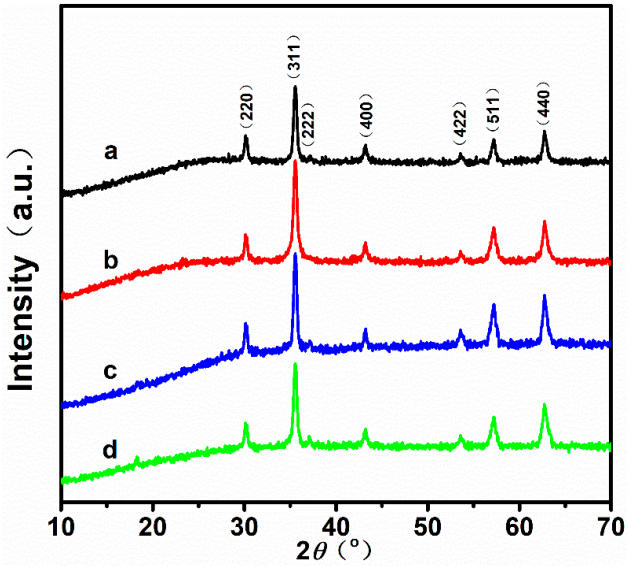

Figure 1. X-ray diffraction patterns of the Fe_3O_4 nanoparticles synthesized by using different ratios of V_{EG}/V_{DEG}: (**a**) 40/60, (**b**) 60/40, (**c**) 80/20, and (**d**) 100/0.

Table 1. Grain size of the samples calculated for the strongest peak (311).

Sample	EG/DEG	Grain Size (nm)
a	40/60	23.62
b	60/40	25.25
c	80/20	25.65
d	100/0	27.86

To confirm the morphology of the samples, we recorded SEM images of the Fe_3O_4 monodispersed nanoparticles, which are shown in Figure 2. The mean diameter of the Fe_3O_4 nanoparticles increased with the increasing ratio of V_{EG}/V_{DEG} during the solvothermal reaction. When the V_{EG}/V_{DEG} was varied from 100/0 to 80/20, 60/40, and 40/60, the average diameters of the resulting Fe_3O_4 nanospheres were approximately 700, 500, 300, and 100 nm, respectively. Additionally, it can be confirmed from the TEM image of Fe_3O_4 nanoparticles shown in Figure 3 that the as-prepared Fe_3O_4 nanospheres are clusters of numerous superfine particles.

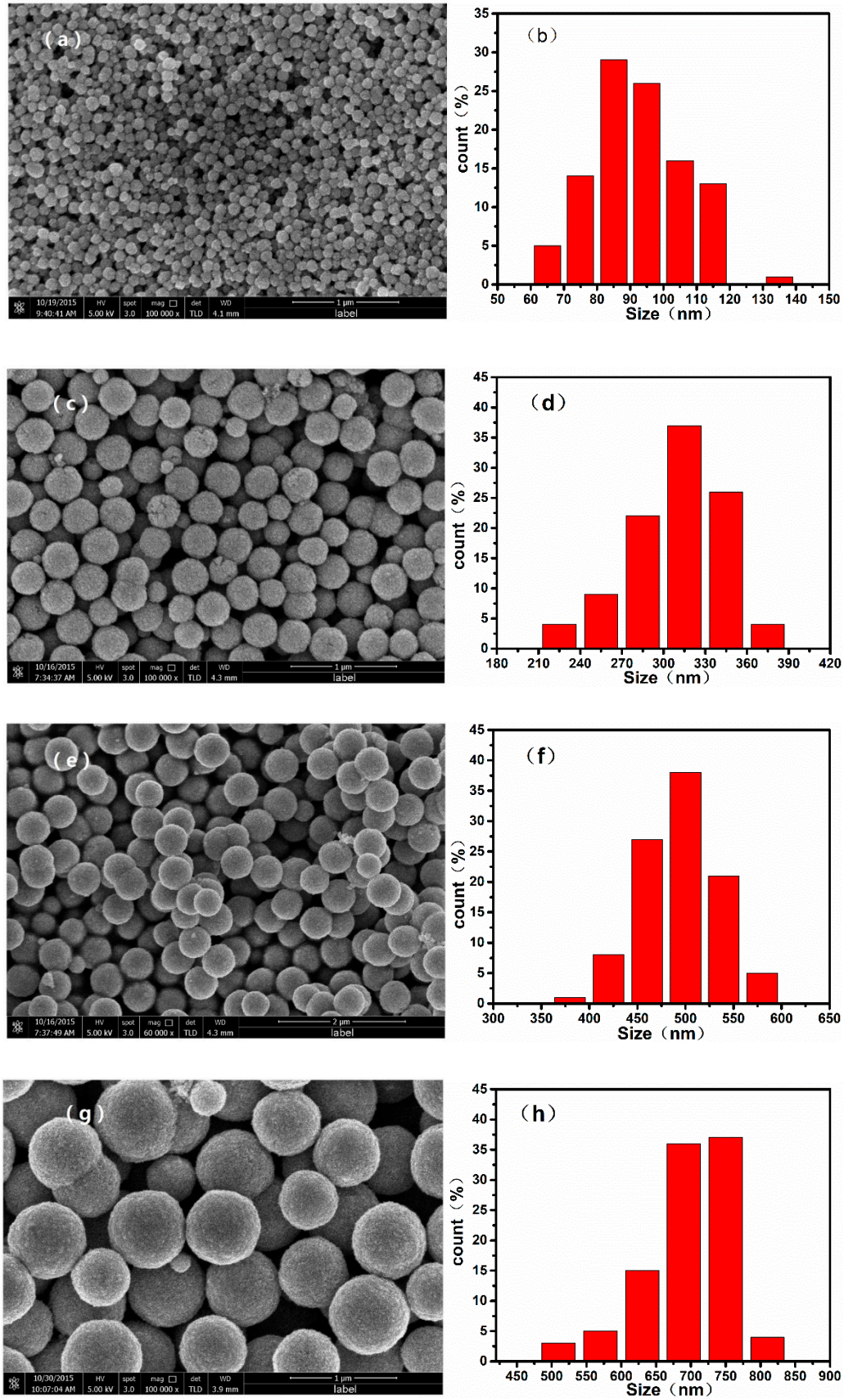

Figure 2. Scanning electron microscope (SEM) images and particle size distribution histograms of Fe_3O_4 nanoparticles synthesized by using different ratios of V_{EG}/V_{DEG}: (**a**), (**b**) 40/60; (**c**), (**d**) 60/40; (**e**), (**f**) 80/20, and (**g**), (**h**) 100/0.

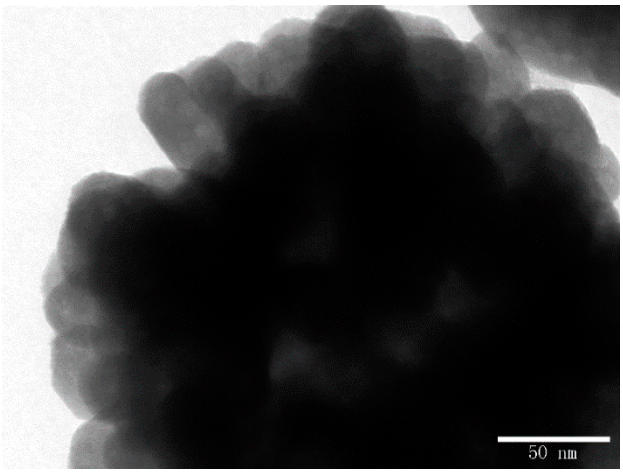

Figure 3. A transmission electron microscope (TEM) image of Fe_3O_4 nanoparticles.

3.2. Magnetic Properties

The room-temperature hysteresis loop of the Fe_3O_4 nanoparticles was measured using a vibrating sample magnetometer (VSM). The magnetization curves of the samples are shown in Figure 4, and the magnetic parameters are listed in Table 2. All Fe_3O_4 nanoparticle samples show excellent superparamagnetic properties with really narrow hysteresis loops. From Table 2, the remanent magnetization (M_r) of Fe_3O_4 nanoparticles with a size of 100, 300, 500, and 700 nm was 3.34, 3.97, 3.26, and 4.28 emu/g, respectively. The saturation magnetization (M_s) of Fe_3O_4 nanoparticles with a size of 100, 300, 500, and 700 nm was 72.14, 75.94, 80.28, and 85.41 emu/g, respectively. In this work, it was further found that the saturation magnetization (M_s) and the remanent magnetization (M_r) can be mildly affected by the size of Fe_3O_4 nanoparticles.

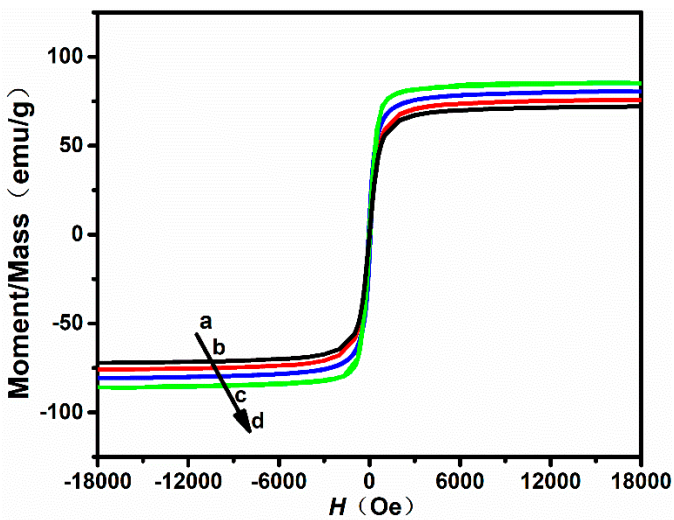

Figure 4. Magnetization hysteresis loops of Fe_3O_4 nanoparticles synthesized by using different ratios of V_{EG}/V_{DEG}: (**a**) 40/6, (**b**) 60/40, (**c**) 80/20, and (**d**) 100/0.

Table 2. Magnetic parameters of the prepared nanoparticles.

Sample	Saturation Magnetization (M_s) emu/g	Remanent Magnetization (M_r) emu/g
a	72.14	3.34
b	75.94	3.97
c	80.28	3.26
d	85.41	4.28

3.3. Formation Mechanism of Fe_3O_4 Nanoparticles with Tunable Sizes

As a typical solvothermal reaction, the formation process of magnetic nanoparticles includes two main steps: nucleation and ripening growth [29]. In this case, the ethylene glycol and diethylene glycol act as the solvent and reductant, respectively, the iron (III) chloride as the iron source, and the sodium acetate (NaAC) provides the hydroxyl-ion and maintains the acid–base equilibrium of the reaction system. The PVP and Na_3Cit are structure guide agents.

As we previously reported [30], during the reaction process, parts of the hydrolyzed Fe^{3+} ions reduce to $Fe(OH)_2$, and combine with the remaining $Fe(OH)_3$ to finally form Fe_3O_4 nanoparticles. As is shown in Figure 5a, the small-molecule citrate groups that have adhered on the magnetic nanocrystals act as both resistance and bridging agents, which prevent the further growth of nanocrystals and agglomerate the neighboring nanocrystals into nanoclusters with low remanent magnetization. As for the PVP long-chain molecules shown in Figure 5b, in the initial process, the macromolecule stabilizers mostly act as bridging agents to guide the neighboring nanocrystals to self-assemble into larger nanoparticles with high saturation magnetization. After the larger nanoparticles are fully covered by the PVP long-chain molecules, the PVP long-chain molecules act as space blocks and prevent the further growth of the nanoparticles. In order to obtain superparamagnetic nanoparticles with high saturation magnetization, the binary Na_3Cit/PVP is added into the reaction system as a structure guide agent.

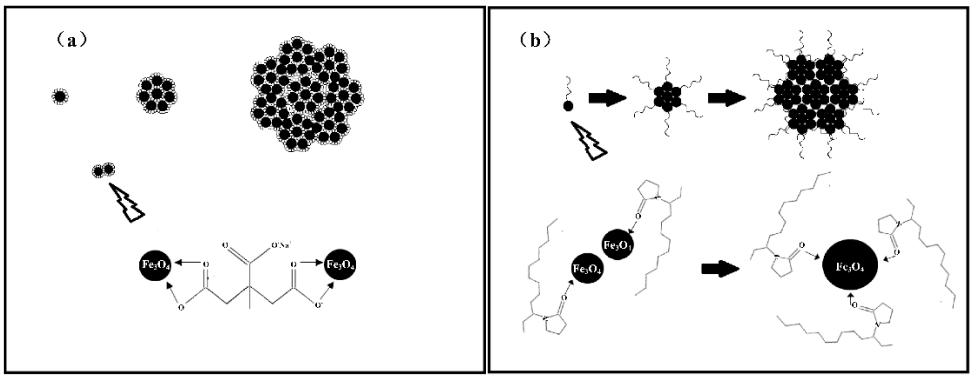

Figure 5. Schematic illustration of the process of obtaining magnetite nanospheres: (**a**) structure guided by sodium citrate (Na_3Cit) and (**b**) structure guided by polyvinyl pyrrolidone (PVP).

In addition, the EG/DEG binary solvent system also plays a key role in controlling the size of the Fe_3O_4 nanoparticles [31]. From the above-mentioned analysis, the formation of magnetic nanoparticles is closely related to the aggregation process. When pure EG is used, the precursor iron alkoxides transform into crystal nuclei and further agglomerate rapidly into large nanoparticles due to their high surface energy. When DEG is added to form a binary solvent with EG, the size of Fe_3O_4 nanoparticles decreases as the V_{EG}/V_{DEG} ratio decreases. DEG forms a more stable coordination iron alkoxide with Fe ions than EG, so the growth rate of Fe_3O_4 grains will slow down, consequently decreasing the size. Furthermore, when EG/DEG coordinates with $FeCl_3$ to form an iron alkoxide, HCl is a byproduct

from the reaction. The accumulation of HCl will inhibit further iron alkoxide formation. When NaAc is introduced, it can react with HCl to reduce the concentration of H^+, and allow the coordination reaction to be completed [32,33].

4. Conclusions

In summary, we have demonstrated a facile synthesis of size-controllable superparamagnetic Fe_3O_4 nanoparticles via a solvothermal method based on an ethylene glycol/diethylene glycol (EG/DEG) binary solvent system. When the V_{EG}/V_{DEG} was varied from 100/0 to 80/20, 60/40, and 40/60, the average diameters of the resulting Fe_3O_4 nanospheres were approximately 700, 500, 300, and 100 nm, respectively. In addition, the saturation magnetization (M_s) of Fe_3O_4 nanoparticles with a size of 100, 300, 500, and 700 nm was 72.14, 75.94, 80.28, and 85.41 emu/g, and the corresponding remanent magnetization (M_r) was 3.34, 3.97, 3.26, and 4.28 emu/g, respectively. These superparamagnetic Fe_3O_4 nanoparticles with high saturation magnetization show outstanding potential as targeted drug carriers.

Author Contributions: Z.Z. conceived and designed the experiments; Y.C. and Z.W. performed the experiments and analyzed the data; J.Z. supervised the entire work. Y.C. wrote the paper.

Funding: This research was funded by the National Natural Science Foundation of China, grant number: 11672041.

Acknowledgments: The authors gratefully acknowledge the support from the State Key Laboratory of Explosion Science and Technology, Beijing Institute of Technology, and the National Natural Science Foundation of China (Grant No. 11672041).

Conflicts of Interest: The authors declare no conflict of interest.

References

1. Mishra, B.; Patel, B.B.; Tiwari, S. Colloidal nanocarriers: A review on formulation technology, types and applications toward targeted drug delivery. *Nanomed.-Nanotechnol. Biol. Med.* **2010**, *6*, 9–24. [CrossRef]
2. Indira, T.K.; Lakshmi, P.K. Magnetic nanoparticles–A review. *Int. J. Pharm. Sci. Nanotechnol.* **2010**, *3*, 1035–1042.
3. Alexiou, C.; Tietze, R.; Schreiber, E.; Jurgons, R.; Richter, H.; Trahms, L.; Rahn, H.; Odenbach, S.; Lyer, S. Cancer therapy with drug loaded magnetic nanoparticles—Magnetic drug targeting. *J. Magn. Magn. Mater.* **2011**, *323*, 1404–1407. [CrossRef]
4. Kumar, A.; Jena, P.K.; Behera, S.; Lockey, R.F.; Mohapatra, S. Multifunctional magnetic nanoparticles for targeted delivery. *Nanomed.-Nanotechnol. Biol. Med.* **2010**, *6*, 64–69. [CrossRef]
5. Dobson, J. Magnetic nanoparticles for drug delivery. *Drug Dev. Res.* **2006**, *67*, 55–60. [CrossRef]
6. Kempe, H.; Kempe, M. The use of magnetite nanoparticles for implant-assisted magnetic drug targeting in thrombolytic therapy. *Biomaterials* **2010**, *31*, 9499–9510. [CrossRef] [PubMed]
7. Wang, M.; Le, H.; Yin, Y. Magnetic field guided colloidal assembly. *Mater. Today* **2013**, *16*, 110–116. [CrossRef]
8. Mody, V.V.; Cox, A.; Shah, S.; Singh, A.; Bevins, W.; Parihar, H. Magnetic nanoparticle drug delivery systems for targeting tumor. *Appl. Nanosci.* **2014**, *4*, 385–392. [CrossRef]
9. Yang, X.Y.; Zhang, X.Y.; Ma, Y.F.; Huang, Y.; Wang, Y.S.; Chen, Y.S. Superparamagnetic graphene oxide–Fe_3O_4 nanoparticles hybrid for controlled targeted drug carriers. *J. Mater. Chem.* **2009**, *19*, 2710–2714. [CrossRef]
10. Padella, F.; Alvani, C.; La, B.A.; Ennas, G.; Liberatore, R.; Varsano, F. Mechanosynthesis and process characterization of nanostructured manganese ferrite. *Mater. Chem. Phys.* **2005**, *90*, 172–177. [CrossRef]
11. Mathur, P.; Thakur, A.; Singh, M. Processing of high density manganese zinc nanoferrites by co-precipitation method. *Z. Phys. Chem.-Int. J. Res. Phys. Chem.* **2007**, *221*, 887–895. [CrossRef]
12. Rondinone, A.J.; Liu, C.; Zhang, Z.J. Determination of magnetic anisotropy distribution and anisotropy constant of manganese spinel ferrite nanoparticles. *J. Phys. Chem. B* **2001**, *10*, 7967–7971. [CrossRef]
13. Bao, N.Z.; Shen, L.M.; Wang, Y.H.; Padhan, P.; Gupta, A. A facile thermolysis route to monodisperse ferrite nanocrystals. *J. Am. Chem. Soc.* **2007**, *129*, 12374–12375. [CrossRef] [PubMed]
14. Gabal, M.A.; Ata-Allah, S.S. Concerning the cation distribution in $MnFe_2O_4$ synthesized through the thermal decomposition of oxalates. *J. Phys. Chem. Solids* **2004**, *65*, 995–1003. [CrossRef]

15. Bai, F.; Wang, D.S.; Huo, Z.Y.; Chen, W.; Liu, L.P.; Liang, X.; Chen, C.; Wang, X.; Peng, Q.; Li, Y.D. A versatile bottom-up assembly approach to colloidal spheres from nanocrystals. *Angew. Chem.-Int. Ed.* **2007**, *46*, 6650–6653. [CrossRef]
16. Xing, Z.; Ju, Z.C.; Yang, J.; Xu, H.Y.; Qian, Y.T. One-step hydrothermal synthesis of $ZnFe_2O_4$ nano-octahedrons as a high capacity anode material for Li-ion batteries. *Nano Res.* **2012**, *5*, 477–485. [CrossRef]
17. Guo, P.Z.; Cui, L.J.; Wang, Y.Q.; Lv, M.; Wang, B.Y.; Zhao, X.S. Facile synthesis of $ZnFe_2O_4$ nanoparticles with tunable magnetic and sensing properties. *Langmuir* **2013**, *29*, 8997–9003. [CrossRef]
18. Xing, R.M.; Lu, L.; Huang, H.P.; Liu, S.H.; Niu, J.Y. Facile Synthesis of Carboxylic Functionalized $MnFe_2O_4$ (M = Mn, Co, Zn) Nanospheres. *J. Nanosci. Nanotechnol.* **2015**, *15*, 5175–5179. [CrossRef]
19. Zhang, Z.L.; Wang, Y.H.; Tan, Q.Q.; Zhong, Z.Y.; Su, F.B. Facile solvothermal synthesis of mesoporous manganese ferrite ($MnFe_2O_4$) microspheres as anode materials for lithium-ion batteries. *J. Colloid Interface Sci.* **2013**, *398*, 185–192. [CrossRef]
20. Chen, G.; Wang, J.Y.; Zhou, L.B.; Ma, W.; Zhang, D.; Ren, F.L.; Yan, H.L.; Qiu, G.Z.; Liu, X.H. A facile solvothermal synthesis and magnetic properties of $MnFe_2O_4$ spheres with tunable sizes. *J. Am. Ceram. Soc.* **2012**, *95*, 3569–3576. [CrossRef]
21. Zheng, H.H.; Zhou, B.F.; Chen, L.; Wang, Y.Q.; Zhang, X.L.; Zhou, S.M. Gel-assisted synthesis of oleate-modified Fe_3O_4@Ag composite microspheres as magnetic SERS probe for thiram detection. *CrystEngComm* **2015**, *17*, 6393–6398. [CrossRef]
22. Zhang, X.L.; Niu, C.Y.; Wang, Y.Q.; Zhou, S.M.; Liu, J. Gel-limited synthesis of dumbbell-like Fe_3O_4-Ag composite microspheres and their SERS applications. *Nanoscale* **2014**, *6*, 12618–12625. [CrossRef] [PubMed]
23. Sun, S.H.; Zeng, H.; Robinson, D.B.; Raoux, S.; Rice, P.M.; Wang, S.X.; Wang, S.X.; Li, G.X. Monodisperse MFe_2O_4 (M = Fe, Co, Mn) Nanoparticles. *J. Am. Chem. Soc.* **2004**, *126*, 273–279. [CrossRef] [PubMed]
24. Jing, X.N.; Liu, T.H.; Wang, D.Q.; Liu, J.; Meng, L.J. Controlled synthesis of water-dispersible and superparamagnetic Fe_3O_4 nanomaterials by a microwave-assisted solvothermal method: From nanocrystals to nanoclusters. *CryStengComm* **2017**, *19*, 5089–5099. [CrossRef]
25. Yan, A.G.; Liu, X.H.; Qiu, G.Z.; Wu, H.Y.; Yi, R.; Zhang, N.; Xu, J. Solvothermal synthesis and characterization of size-controlled Fe_3O_4 nanoparticles. *J. Alloys Compd.* **2008**, *458*, 487–491. [CrossRef]
26. Li, L.; Yang, Y.; Ding, J.; Xue, J.M. Synthesis of magnetite nanooctahedra and their magnetic field-induced two-/three-dimensional superstructure. *Chem. Mater.* **2010**, *22*, 3183–3191. [CrossRef]
27. Kovalenko, M.V.; Bodnarchuk, M.I.; Lechner, R.T.; Hesser, G.; Schaffler, F.; Heiss, W. Fatty acid salts as stabilizers in size-and shape-controlled nanocrystal synthesis: The case of inverse spinel iron oxide. *J. Am. Chem. Soc.* **2007**, *129*, 6352–6353. [CrossRef]
28. Redl, F.X.; Black, C.T.; Papaefthymiou, G.C.; Sandstrom, R.L.; Yin, M.; Zeng, H.; Murray, C.B.; O'Brien, S.P. Magnetic, electronic, and structural characterization of nonstoichiometric iron oxides at the nanoscale. *J. Am. Chem. Soc.* **2004**, *126*, 14583–14599. [CrossRef]
29. Duan, L.F.; Wang, Y.X.; Wang, L.N.; Zhang, F.F.; Wang, L.M. Mesoporous MFe_2O_4 (M = Mn, Co, and Ni) for anode materials of lithium-ion batteries: Synthesis and electrochemical properties. *Mater. Res. Bull.* **2015**, *61*, 195–200. [CrossRef]
30. Li, S.C.; Zhang, T.L.; Tang, R.Z.; Qiu, H.; Wang, C.Q.; Zhou, Z.N. Solvothermal synthesis and characterization of monodisperse superparamagnetic iron oxide nanoparticles. *J. Magn. Magn. Mater.* **2015**, *379*, 226–231. [CrossRef]
31. Xuan, S.H.; Wang, F.; Wang, Y.X.J.; Yu, J.C.; Leung, K.C.F. Facile synthesis of size-controllable monodispersed ferrite nanospheres. *J. Mater. Chem.* **2010**, *20*, 5086–5094. [CrossRef]
32. Zhong, L.S.; Hu, J.S.; Liang, H.P.; Cao, A.M.; Song, W.G.; Wan, L.J. Self-Assembled 3D flowerlike iron oxide nanostructures and their application in water treatment. *Adv. Mater.* **2006**, *18*, 2426–2431. [CrossRef]
33. Larcher, D.; Sudant, G.; Patrice, R.; Tarascon, J.M. Some insights on the use of polyols-based metal alkoxides powders as precursors for tailored metal-oxides particles. *Chem. Mater.* **2003**, *15*, 3543–3551. [CrossRef]